

Application of Supercritical CO₂ in Nuclear Energy Systems

Michael Podowski

Workshop on Supercritical Carbon Dioxide and
Material Interactions
Brookhaven National Laboratory
March 21-23, 2011



Outline

- Background
- Application of supercritical fluids in nuclear energy systems
- Generic issues associated with supercritical fluid systems
- Recent advancements in the state-of-the-art in Supercritical Fluid Science and Engineering

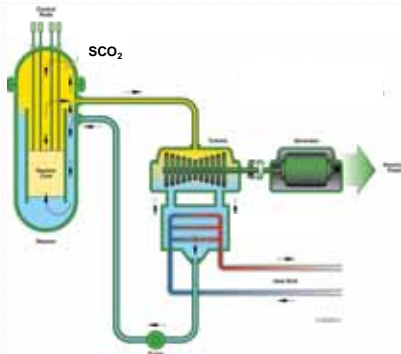


Background

- Supercritical carbon dioxide (S-CO₂) is a very promising material for future applications encompassing a broad spectrum of fields and industries
- Possible applications include:
 - the use of S-CO₂ as a working fluid in Gen. IV reactors: either as reactor coolant in the Supercritical CO₂ Reactor (SCO₂R), or as secondary-system coolant in the Sodium Fast Reactor (SFR) with S-CO₂ Brayton Cycle
 - the use nuclear power for CO₂ sequestration and heavy oil extraction



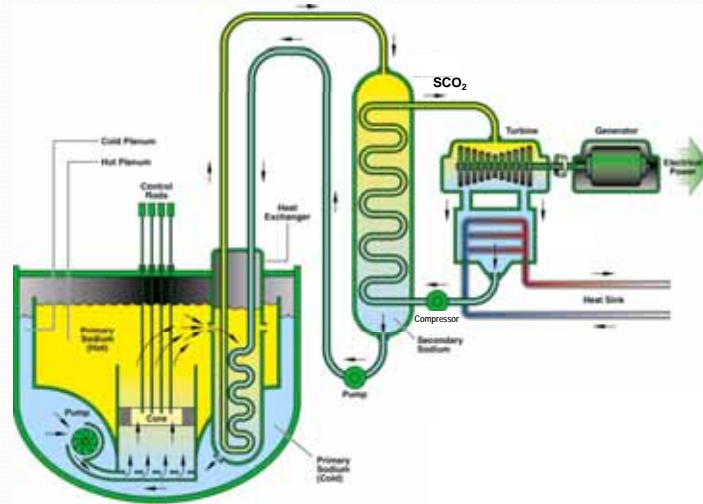
Supercritical CO₂ Reactor (S-CO₂R)



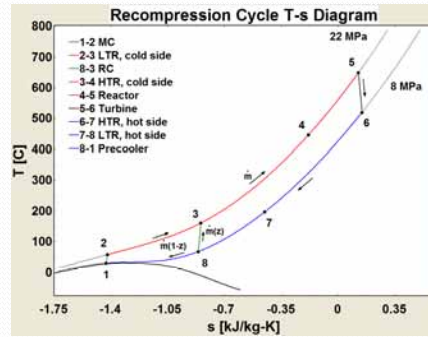
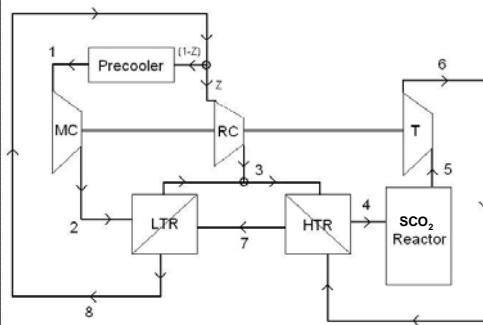
- Advantages:
 - direct thermodynamic cycle
 - high efficiency
- Unresolved issues
 - effect of radiation on materials at high temperature
 - core neutronics (thermal vs. fast)
 - core heat transfer
 - flow-induced instabilities
 - accident mitigation



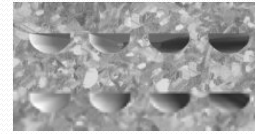
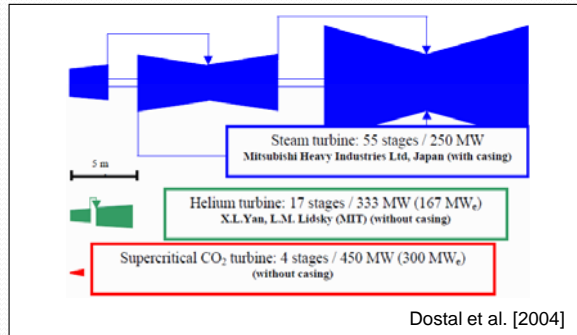
Sodium Fast Reactor (SFR) with S-CO₂ Brayton Cycle



SCO₂ Brayton Cycle



Advantages of Supercritical CO₂ Brayton Cycle



Printed Circuit Heat Exchanger (PCHE)

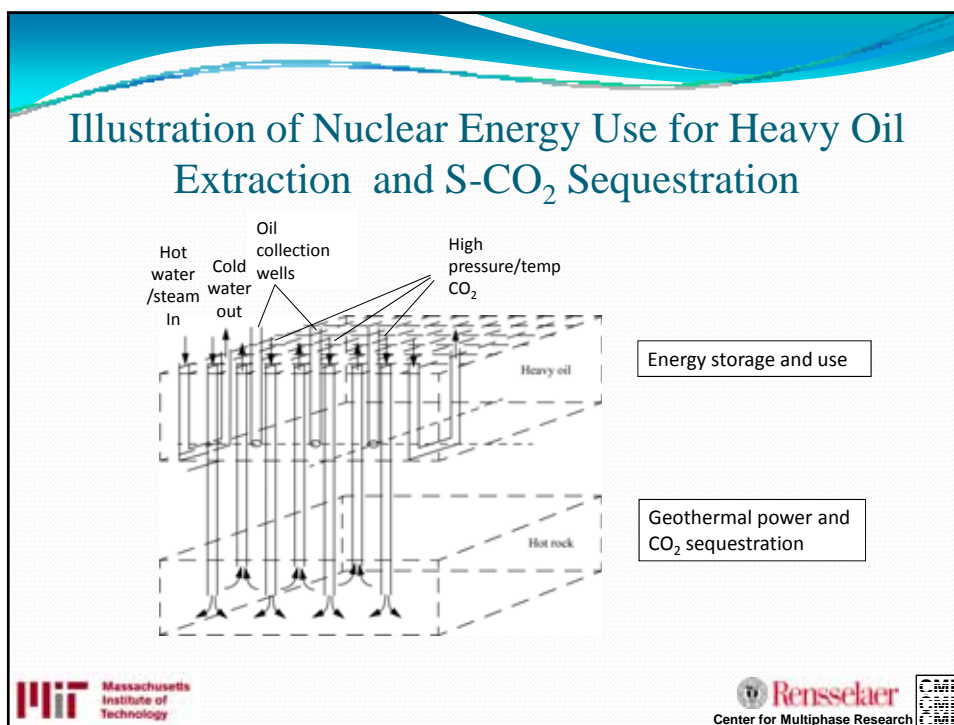
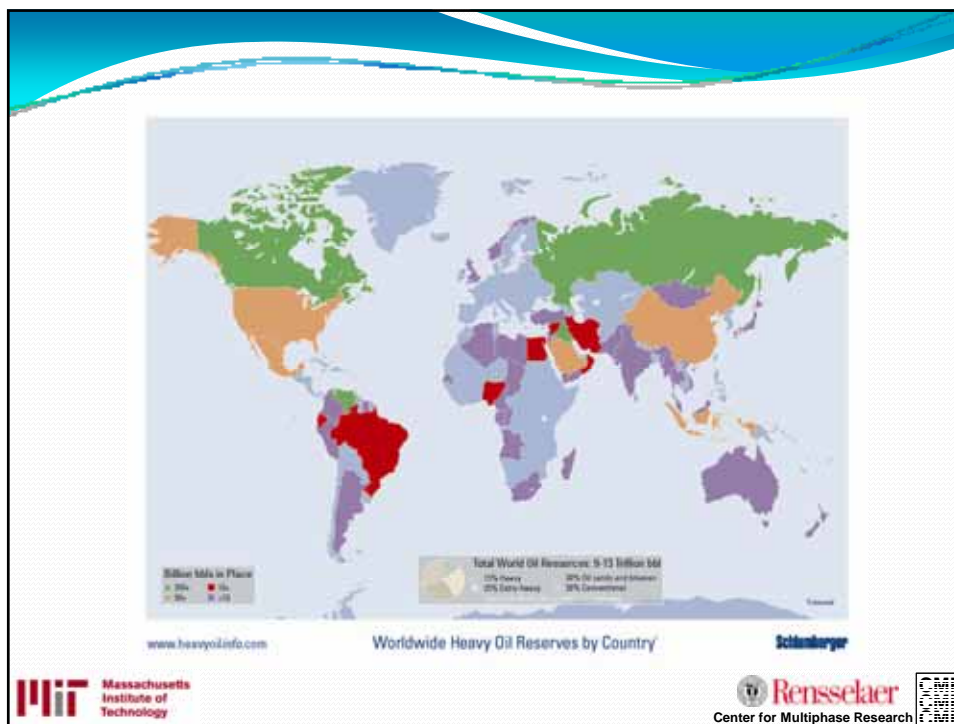


PCHE and shell and tube heat exchangers with equal power

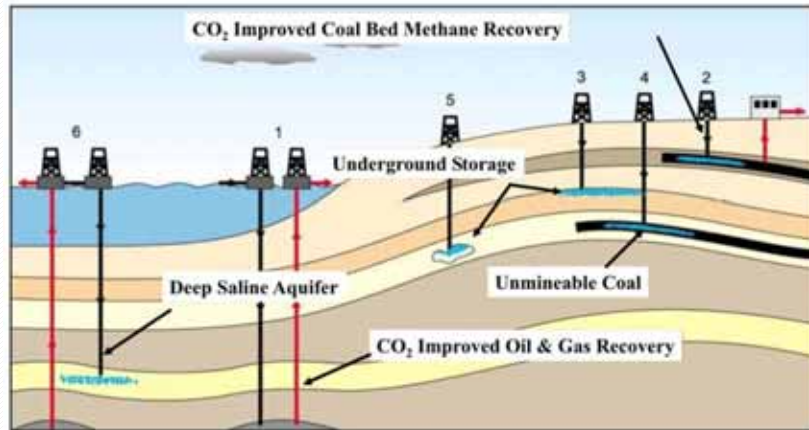
- Size reduction of turbo-machinery
- Good properties of SCO₂ as reactor coolant
- High efficiency of thermodynamic cycle

Geological Applications of Nuclear Energy

- Characteristic features of nuclear power systems
 - practical limits on thermodynamic cycle efficiency: 50% or less
 - potential under utilization during low demand periods
- Future utilizations of available thermal and electric energy
 - hot water/steam from NPP heat rejection systems can be injected into underground layers of heavy-oil-rich sandstone
 - use of electricity during low demand periods for S-CO₂ injection into deep oil and gas deposits and into heavy rock beds (sequestration)



Geological Options for CO₂ Use and Sequestration



Modified from <http://www.spacedaily.com/news/greenhouse-00j.html>



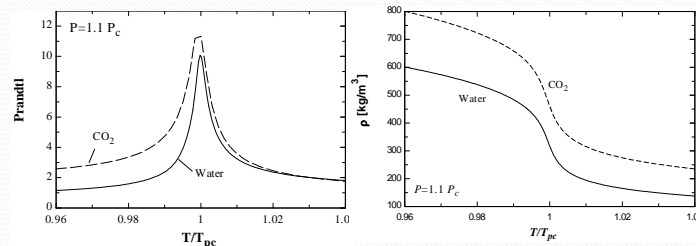
Generic Issues associated with Supercritical Fluid Systems

- Fluid mechanics of variable-property fluid flow in complex geometries (compressors, mixing in large volumes)
- Heat transfer (enhancement, deterioration)
- Flow induced instabilities



Key Characteristics of Supercritical Fluids

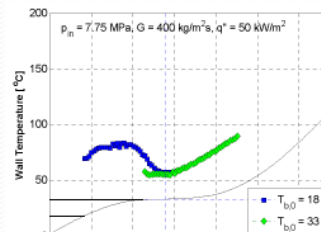
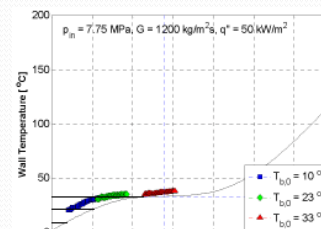
- No phase change
- High temperature and thermodynamic cycle efficiency
- **Dramatic changes in fluid properties in the pseudo-critical region**

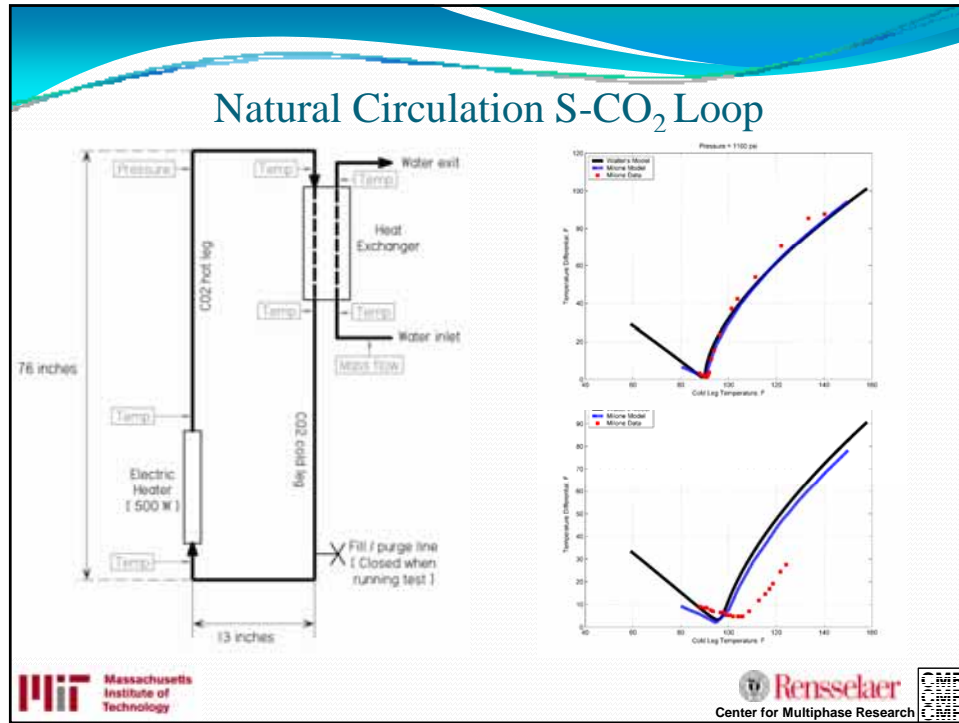


Normalized properties of water and CO₂ at supercritical pressures

Heat Transfer at Supercritical Conditions

- Heat transfer enhancement occurs throughout the pseudo-critical region for low heat flux and high mass flow rates
- Heat transfer degradation occurs at high heat flux and/or low mass flow rates





Recent Advancements in the Analysis of Thermo-Fluid Phenomena in Supercritical Fluid Systems

- Multidimensional CFD modeling and simulations of fluid flow and heat transfer in heated channels
- Flow-induced instabilities in parallel-channel systems
- Current studies include the modeling of S-CO₂ compressors and loop dynamics and stability

Turbulence Modeling at Supercritical Pressures

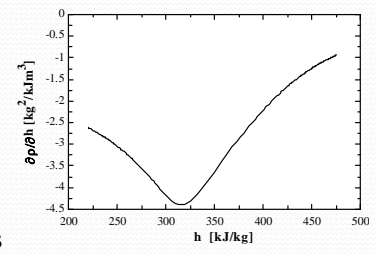
- Conservation of mass

$$\frac{\partial(\bar{\rho})}{\partial t} + \nabla \cdot (\bar{\rho} \bar{\mathbf{u}}) + \nabla \cdot (\overline{\rho' \mathbf{u}'}) = 0$$
- Conservation of momentum

$$\frac{\partial(\rho \mathbf{u})}{\partial t} + \nabla \cdot (\rho \mathbf{u} \mathbf{u}) = -\nabla P + \nabla \cdot \boldsymbol{\tau} + \rho \mathbf{F}$$
- For turbulent flows with variable properties

$$\nabla \cdot (\rho \mathbf{u} \mathbf{u}) = \frac{\partial}{\partial x_j} (\overline{\rho u_i u_j} + \overline{\rho u'_i u'_j} + \overline{\rho' u'_i u_j} + \overline{\rho' u'_j u_i} + \overline{\rho' u'_i u'_j})$$

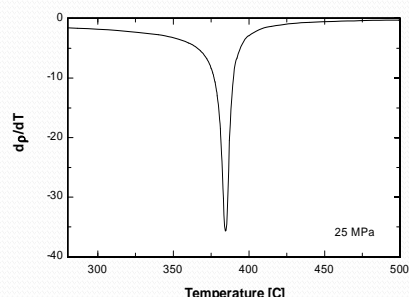
where $\overline{\rho' u'_i} = \frac{\partial \rho}{\partial h} \Big|_{\bar{h}} \overline{h' u'_i}$
- Therefore derivatives in fluid properties may play an important role in turbulence modeling



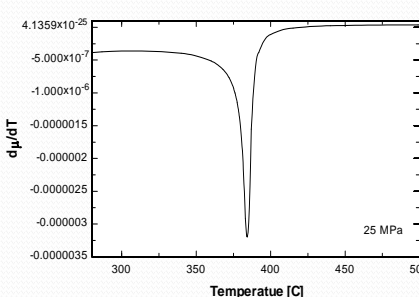
A line graph showing the derivative of density with respect to enthalpy, $\partial \rho / \partial h$ in units of $\text{kg}^{-2} / \text{kJ m}^3$, plotted against enthalpy h in kJ/kg . The x-axis ranges from 200 to 500, and the y-axis ranges from -4.5 to 0. The curve shows a sharp negative peak around $h = 320$ kJ/kg , reaching approximately -4.2.



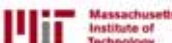

Derivatives of physics properties

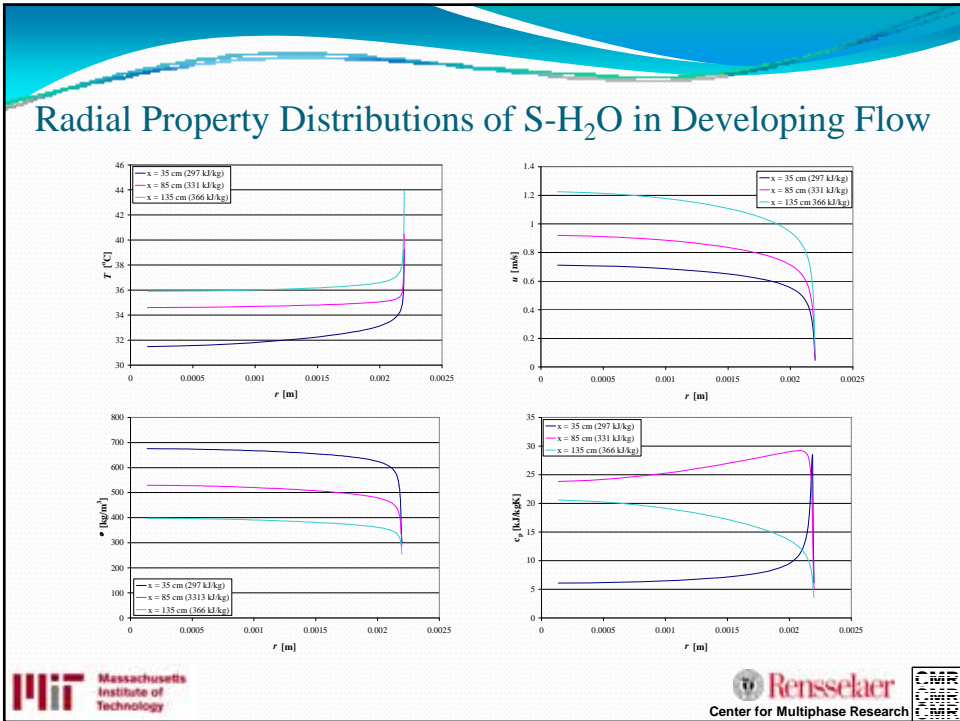
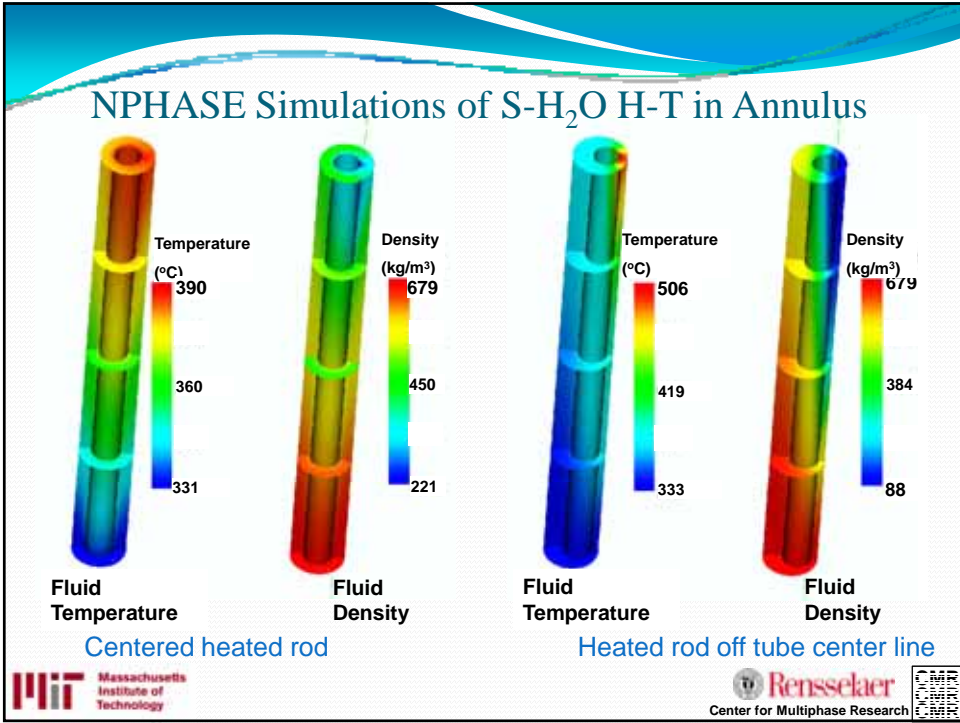


Graph of $d\rho/dT$ vs Temperature [C] at 25 MPa. The x-axis ranges from 300 to 500, and the y-axis ranges from -40 to 0. The curve shows a sharp negative peak around 380°C, reaching approximately -35.

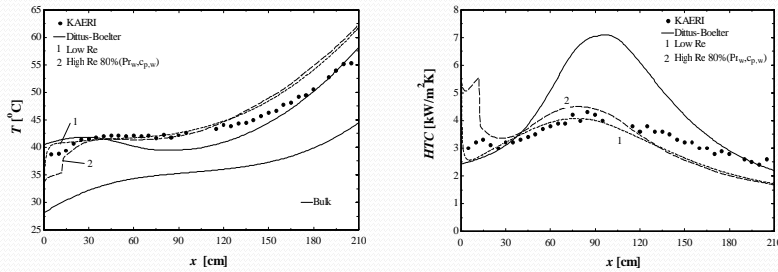


Graph of $d\rho/dT$ vs Temperature [C] at 25 MPa. The x-axis ranges from 300 to 500, and the y-axis ranges from -0.0000035 to 4.1359×10^{-25} . The curve shows a sharp negative peak around 380°C, reaching approximately -0.0000035 .



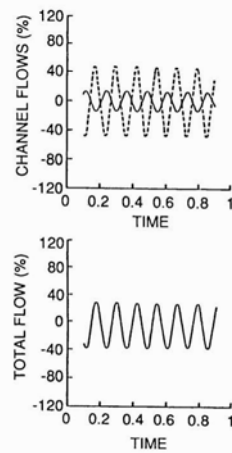
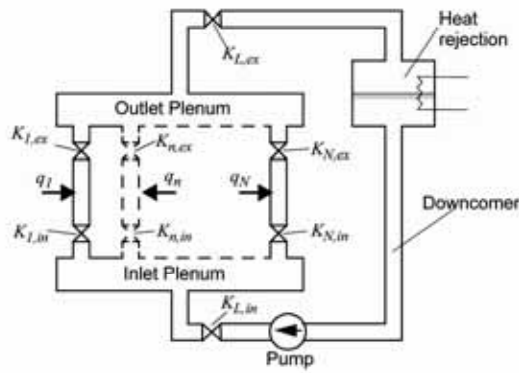
Predictions of Heat Transfer S-H₂O



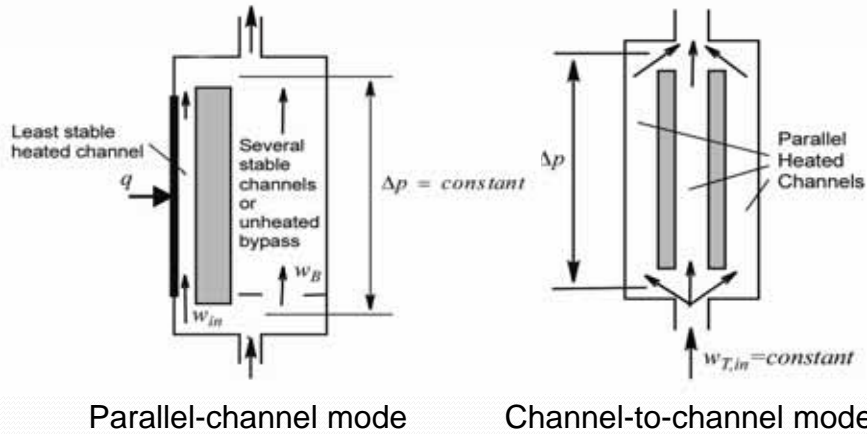
- Low-Reynolds Model predicts wall temperature through pseudo-critical region better than High-Reynolds model
- Predicted wall temperature after pseudo-critical region is slightly higher than experimental data
- Effects of property variations on heat and mass transfer play a key role throughout boundary layer region



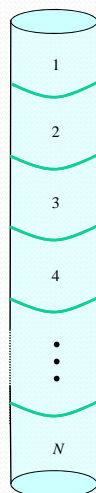
Flow-Induced Instabilities



Stability Analysis of Supercritical Fluid Systems



Method-1: Channel Discretization



- Continuity and energy equations are discretized

$$A_n \frac{d\bar{y}_n}{dt} + \frac{(x_n - x_{n-1})}{\Delta z} = 0$$

$$\rho_{ss,n} \frac{d\bar{y}_n}{dt} + b \left(\frac{x_n + x_{n-1}}{2} \right) + G_{ss} \frac{(y_n - y_{n-1})}{\Delta z} = 0$$

where $\begin{cases} x_n = \delta G(t, z_n) \\ y_n = \delta h(t, z_n) \end{cases}$

- After algebraic manipulations and including the momentum equation

$$\frac{dy_n}{dt} = \lambda_n x_0 + \gamma_{n,1} y_1 + \gamma_{n,2} y_2 + \dots + \gamma_{n,n} y_n$$

$$\frac{dx_0}{dt} = \psi \delta \Delta P + \beta x_0 + \alpha_1 y_1 + \alpha_2 y_2 + \dots + \alpha_N y_N$$

where $x_0 = \delta G_{in}(t)$

$$x_0^{(N)} + a_{N-1} x_0^{(N-1)} + \dots + a_1 x_0 + a_0 = \psi \delta \Delta P$$



Method 2: Direct Frequency-Domain Solution

- Taking $s = j\omega$, the real and imaginary components of individual variables are separated, e.g., $\hat{X}(j\omega) = \hat{X}_R(\omega) + j\hat{X}_I(\omega)$

$$\begin{aligned} \frac{d^2 \hat{X}_R}{dz^2} - \beta \frac{d\hat{X}_R}{dz} - \alpha(z)\omega \frac{d\hat{X}_I}{dz} + \gamma(z)\omega \hat{X}_I &= 0 & \omega \hat{Y}_R &= -\frac{1}{A} \frac{d\hat{X}_I}{dz} \\ \frac{d^2 \hat{X}_I}{dz^2} + \alpha(z)\omega \frac{d\hat{X}_R}{dz} - \beta \frac{d\hat{X}_I}{dz} - \gamma(z)\omega \hat{X}_R &= 0 & \omega \hat{Y}_I &= \frac{1}{A} \frac{d\hat{X}_R}{dz} \end{aligned}$$

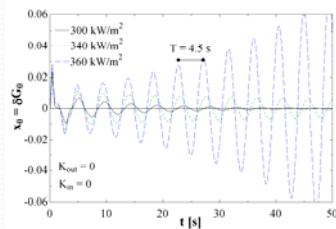
$$\begin{aligned} \left[\frac{\delta \Delta P}{X_0} \right]_R &= -\omega \int_0^L \hat{X}_I dz + \frac{2G_{ss}}{\rho_{ss,L}} \hat{X}_R - \frac{G_{ss}^2 A_{L1}}{(\rho_{ss,L})^2} \hat{Y}_R - \frac{2G_{ss}}{\rho_{ss,0}} + \int_0^L [C_1 \hat{X}_R + C_2 \hat{Y}_R] dz + g \int_0^L A \hat{Y}_R dz + K_{in} \frac{G_{ss}}{\rho_{ss,0}} + K_{out} \left(\frac{G_{ss}}{\rho_{ss,L}} \hat{X}_R - \frac{G_{ss}^2 A_{L1}}{2(\rho_{ss,L})^2} \hat{Y}_R \right) \\ \left[\frac{\delta \Delta P}{X_0} \right]_I &= \omega \int_0^L \hat{X}_R dz + \frac{2G_{ss}}{\rho_{ss,L}} \hat{X}_I - \frac{G_{ss}^2 A_{L1}}{(\rho_{ss,L})^2} \hat{Y}_I + \int_0^L [C_1 \hat{X}_I + C_2 \hat{Y}_I] dz + g \int_0^L A \hat{Y}_I dz + K_{out} \left(\frac{G_{ss}}{\rho_{ss,L}} \hat{X}_I - \frac{G_{ss}^2 A_{L1}}{2(\rho_{ss,L})^2} \hat{Y}_I \right) \end{aligned}$$

- Characteristic function of the system becomes

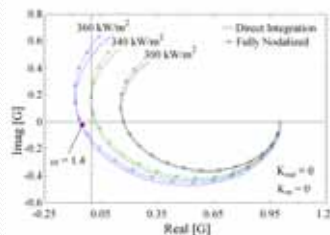
$$G(j\omega) = \frac{\delta \Delta P(j\omega)}{X_0(j\omega)} = \text{Re } G(\omega) + j \text{Im } G(\omega)$$



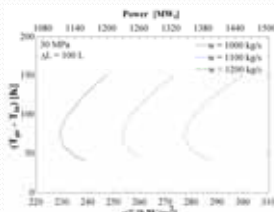
1-D Simulation of Flow-Induced Oscillations



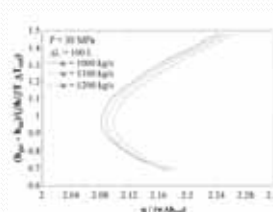
Time-domain



Frequency-domain



Dimensional stability map



Nondimensional stability map



Current Research Directions - Fundamentals

- Impact of variable fluid properties on kinematic and thermal aspects of turbulence in S-C fluids
- Importance of multidimensional phenomena on dynamics of S-C fluid systems
- Stability analysis of closed-loop systems
- Modeling of fluid flow and heat transfer in large systems (mechanistic approach to porous media)

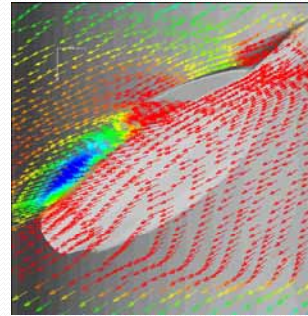
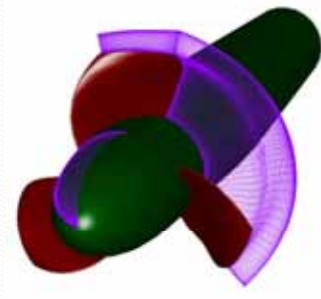
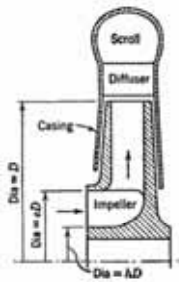


Practical Applications of Fundamental Research

- S-C Brayton cycle:
 - Heat exchangers
 - Flow in complex geometries (compressors)
- Flow-induced instabilities in closed-loop heat transport systems



Illustration: NPHASE-CMFD Simulation of Flow in Rotating Machinery



Potential Future Applications

- Efficient methods of analysis to understand S-CO₂ behavior in deep geological deposits:
 - oil extraction
 - sequestration



Thank you for your attention!



Massachusetts
Institute of
Technology



Rensselaer

Center for Multiphase Research

